When Semantics Connect the Swarm: LLM-Driven Fuzzy Control for Cooperative Multi-Robot Underwater Coverage

Jingzehua Xu[1,†], *Student Member, IEEE*, Weihang Zhang[2,†], Yangyang Li[3,†], Hongmiaoyi Zhang[4]
Guanwen Xie[1], *Student Member, IEEE*, Jiwei Tang[5], *Student Member, IEEE*,
Shuai Zhang[6], *Member, IEEE*, and Yi Li[1,✉], *Member, IEEE*

***Abstract*—Underwater multi-robot cooperative coverage remains challenging due to partial observability, limited communication, environmental uncertainty, and the lack of access to global localization. To address these issues, this paper presents a semantics-guided fuzzy control framework that couples Large Language Models (LLMs) with interpretable control and lightweight coordination. Raw multimodal observations are compressed by the LLM into compact, human-interpretable semantic tokens that summarize obstacles, unexplored regions, and Objects Of Interest (OOIs) under uncertain perception. A fuzzy inference system with pre-defined membership functions then maps these tokens into smooth and stable steering and gait commands, enabling reliable navigation without relying on global positioning. Then, we further coordinate multiple robots by introducing semantic communication that shares intent and local context in linguistic form, enabling agreement on who explores where while avoiding redundant revisits. Extensive simulations in unknown reef-like environments show that, under limited sensing and communication, the proposed framework achieves robust OOI-oriented navigation and cooperative coverage with improved efficiency and adaptability, narrowing the gap between semantic cognition and distributed underwater control in GPS-denied, map-free conditions.**

***Index Terms*—Large Language Model, Semantic Communication, Fuzzy Control, Multi-Robot System, Underwater Coverage.**

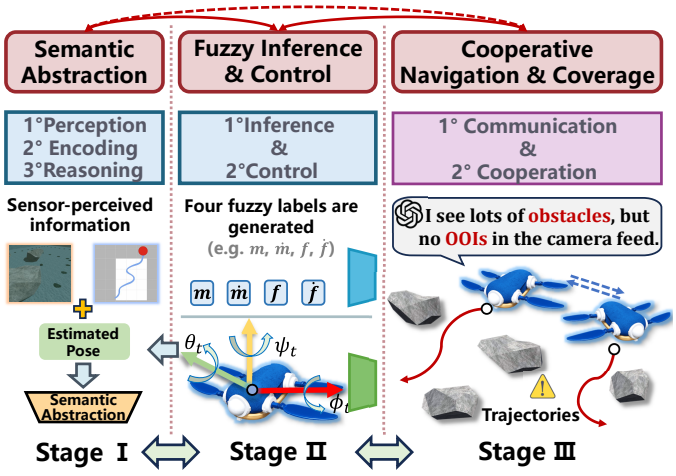

Fig. 1. **Schematic illustration of the proposed semantics-guided fuzzy control framework**, comprising Semantic Abstraction, Fuzzy Inference & Control, and Cooperative Navigation & Coverage, which together enable intelligent perception, decision-making, and coordination among multiple robots in the underwater coverage task.

I. INTRODUCTION

Underwater multi-robot cooperative coverage is a fundamental capability for tasks such as ecological patrol, pipeline inspection, coral reef assessment, and underwater heritage exploration [1], [2], with broad potential in deep-sea resource development, infrastructure maintenance, and large-scale ecological monitoring [3], [4]. Unlike terrestrial and aerial environments, underwater settings impose distinct constraints: optical imaging rapidly degrades due to absorption and scattering [5], [6], leading to partial observability and highly uncertain perception; acoustic sensing suffers from multipath interference and ambient noise [7], [8], which severely limits inter-robot communication bandwidth and reliability; and local flow fields are highly dynamic, inducing strong coupling between propulsion posture and trajectory control [9], [10]. Moreover, the unstructured environment—with irregular seabed terrain, vegetation, suspended particles, and moving obstacles such as fish schools or drifting debris—constantly reshapes navigable space [1], [11], intensifying environmental uncertainty and reducing the predictability of local motion patterns. In addition, the lack of access to global localization or prior environmental maps forces each robot to rely solely on local sensing and dead reckoning for navigation, making cooperative coverage and spatial coordination even more difficult. Consequently, achieving distributed cooperation with high coverage, low redundancy, and strong adaptability in such partially observable, communication-constrained, and GPS-denied underwater environments remains a central challenge in mobile computing and edge intelligence. [12], [13].

To address these challenges, coverage research mainly falls into three directions. The first is geometry- and topology-based planning, including grid sweeping, boustrophedon de-

[1]J. Xu, G. Xie and Y. Li are with Tsinghua Shenzhen International Graduate School, Tsinghua University, Shenzhen, 518055, China, and with Department of Engineering, University of Cambridge, CB2 1PZ, United Kingdom. E-mail: 19955778426@163.com, xgw24@mails.tsinghua.edu.cn, liyi@sz.tsinghua.edu.cn.
[2]W. Zhang is with Department of Electrical and Computer Engineering, Duke University, Durham, NC 27708, USA. E-mail: weihang.zhang@duke.edu.
[3]Y. Li is with Electrical Engineering & Computer Science Department, Massachusetts Institute of Technology, Cambridge, MA 02139, USA. E-mail: annieliy@mit.edu.
[4]H. Zhang is with School of Automation Science and Engineering, South China University of Technology, Guangzhou, 510641, China. E-mail: 202511084270@mail.scut.edu.cn.
[5]J. Tang is with Department of Data and Systems Engineering, The University of Hong Kong, Hong Kong, 999077, China, E-mail: tangjiwei7@gmail.com.
[6]S. Zhang is with Department of Data Science, New Jersey Institute of Technology, NJ 07102, USA. E-mail: sz457@njit.edu.
† These authors contributed equally to this work.
✉ Corresponding author.

composition, and frontier exploration [14], [15], which depend on stable maps and accurate localization. The second is distributed optimization and consensus control, such as potential fields, Voronoi partitioning, and task allocation [12], [16], which requires continuous information exchange for convergence. The third is learning-based approaches, such as Reinforcement Learning (RL) and imitation learning, which pursue adaptability under partial observability via end-to-end policies [17], [18], [19]. However, all face persistent bottlenecks underwater: unreliable mapping or lack of access to global localization degrades geometry-based methods [3], [15]; limited communication constrains distributed optimization [16], [12]; and learning-based methods demand extensive data while lacking interpretability, transferability, and robustness under perception degradation and environmental uncertainty [17], [20]. Although some distributed methods enable multi-robot cooperation, most still rely on frequent numerical exchanges, resulting in low efficiency under communication-constrained conditions [7], [8]. These limitations motivate a semantics-driven cooperation mechanism that sustains swarm coordination and enhances understanding of the dynamic and uncertain underwater environments, even with limited inter-robot communication.

Building on these limitations, recent research has shifted toward semantic or task-oriented coordination, which extracts and transmits only the most relevant environmental information for decision-making under uncertainty [21], [22]. Beyond improving communication efficiency, this paradigm enhances environmental understanding and situational awareness, enabling agents to interpret dynamic underwater scenes more effectively [23], [24]. In this context, Large Language Models (LLMs) have become powerful tools for semantic abstraction and reasoning, showing strong cross-modal generalization across visual, sonar, and inertial data [25], [26]. By compressing noisy sensory inputs into structured, high-level representations—such as "obstacles ahead" or "dense Objects Of Interest (OOIs) on the left"—LLMs allow robots to reason beyond raw perception, improving adaptability in uncertain environments [27]. However, semantics alone are insufficient: directly mapping LLM-derived descriptions to control actions can lead to opaque "black-box" behavior [28]. Robust multi-robot cooperation further requires interpretable and adaptive control mechanisms that translate semantic understanding into coherent swarm behaviors [19], [29]. To this end, integrating semantic reasoning with interpretable control mechanisms is essential for enabling underwater swarms to maintain coordination and adapt to uncertain environments.

Based on the above analysis, this paper presents a semantics-guided fuzzy control framework for multi-bionic turtle platforms that employ fin- or paddle-based propulsion and exhibit high maneuverability and fine-grained control, enabling efficient coverage operations in partially observable underwater environments [30], [31]. In this framework, LLMs guided by tailored prompts convert high-dimensional multimodal sensor data into compact, interpretable semantic tokens, reducing redundancy and enhancing contextual understanding for decision-making. These semantic tokens are then processed through a fuzzy inference system with expert-informed rules and pre-defined membership functions, mapping linguistic inputs to smooth and robust control actions under dynamic conditions. Furthermore, an LLM-driven semantic communication mechanism enables efficient multi-robot cooperation by sharing intent and context tokens instead of raw data, ensuring scalable, context-aware coordination even under communication constraints and environmental uncertainty.

In summary, the main contributions of this paper are listed as follows:

- **LLM-Guided Efficient Semantic Abstraction**: We introduce a semantic perception paradigm in which LLMs are guided through carefully designed prompts to transform high-dimensional multimodal sensory inputs into compact, interpretable semantic representations. This abstraction significantly reduces data redundancy and enhances contextual understanding for downstream decision-making in uncertain underwater environments.
- **Fuzzy Inference System and Controller Design**: Building on the compact, interpretable semantics produced by the LLM layer, we develop a fuzzy inference system with expert-informed rules and pre-defined membership functions that map linguistic cues to continuous control commands. This controller operationalizes high-level intent into smooth and robust actuation while remaining transparent and easily auditable/tunable for diverse tasks and underwater conditions.
- **LLM-Driven Semantic Communication for Cooperative Swarms**: Furthermore, we design an LLM-driven semantic communication mechanism that enables efficient multi-robot collaboration. Each robot shares compact, interpretable intent and context tokens generated by the LLM, allowing others to infer objectives and environmental understanding without transmitting raw sensory data. This semantics-centered approach enhances cooperative efficiency, enabling the multi-robot system to coordinate tasks and maintain coherent behavior, even under limited connectivity and uncertain underwater conditions.
- **Comprehensive High-Fidelity Evaluation**: We validate the proposed framework through extensive Webots-based simulations with multi-bionic turtle swarms performing underwater coverage tasks, demonstrating superior coverage efficiency, stable performance under perception uncertainty, and strong cross-environment generalization.

The remainder of this paper is organized as follows: Section II reviews related work on underwater multi-robot cooperative coverage, while Section III details the methodology of this work. Section IV describes the simulation experiments and the experimental results. Finally, Section V concludes the paper and outlines current limitations and future directions.

II. RELATED WORK

This section reviews prior research most relevant to our work, organized into four directions: (A) Foundations of Underwater Coverage, (B) Semantic and Task-Oriented Coordination for Underwater Swarms, and (C) Interpretable and Fuzzy Control for Robust Multi-Robot Systems.

A. Foundations of Underwater Coverage

Classical underwater coverage approaches primarily rely on geometry- and topology-based planning. Galceran *et al*. [14] conducted a comprehensive survey of coverage algorithms, such as grid sweeping, boustrophedon decomposition, and frontier exploration, emphasizing their reliance on stable maps and accurate localization. Ma *et al*. [15] proposed a coverage path planning method for an autonomous underwater helicopter, integrating boustrophedon motion with VFH+-based obstacle avoidance using single-beam sonar. However, these methods assume reliable perception, which is rarely valid under dynamic underwater conditions. Zeng *et al*. [5] and Jaffe [6] reported that optical imaging rapidly deteriorates due to light absorption and scattering, while Li *et al*. [7] and Huang *et al*. [8] demonstrated that acoustic sensing suffers from multipath interference and Doppler distortion. Furthermore, Gbison *et al*. [10] revealed that unsteady hydrodynamic forces tightly couple posture and trajectory, making control increasingly difficult in unstructured environments [11].

To improve scalability and autonomy, Ren *et al*. [16] proposed a consensus-seeking strategy with convergence guarantees under dynamic topologies, while Cao *et al*. [12] summarized distributed coordination schemes—such as potential fields, Voronoi partitioning, and task allocation—that enable decentralized cooperation. Despite their success, these frameworks require continuous numerical exchanges, limiting efficiency under bandwidth-constrained underwater communication [7], [8]. To enhance adaptability, Nguyen *et al*. [17] introduced deep multi-agent RL for cooperative control, and Sebastián *et al*. [19] further presented a physics-informed multi-robot RL method enabling scalable and energy-consistent distributed control. Arulkumaran *et al*. [18] and Zhu *et al*. [20] discussed the challenges of generalization and transferability in uncertain environments. Nevertheless, these learning-based methods often demand large amounts of data and lack interpretability and robustness, motivating the development of more compact, context-aware coordination frameworks that maintain cooperation and adaptability in unknown underwater environments with minimal inter-robot communication.

B. Semantic and Task-Oriented Coordination for Underwater Swarms

To overcome the perception and communication bottlenecks of traditional coordination frameworks, recent research has turned toward semantic or task-oriented mechanisms that focus on transmitting only decision-relevant information. Li *et al*. [21] highlighted the shift from the Shannon paradigm to semantic communication, which transmits meaning instead of symbols for more efficient and sustainable wireless networks amid rising Internet of things demands, while Zhang *et al*. [22] conducted a comprehensive review outlining its potential for intelligent multi-agent systems. In the underwater domain, Chen *et al*. [23] proposed an LLM-based semantic communication framework for underwater images, enabling efficient and robust transmission via semantic compression. Additionally, Qin *et al*. [24] designed a physics-guided semantic communication method for underwater transmission. Collectively, these approaches highlight the shift from raw data transmission to knowledge-centric coordination, improving the system's resilience and perceptual awareness under environmental uncertainty in underwater scenarios.

Beyond efficiency, semantics enhance environmental understanding and adaptive reasoning. Otter *et al*. [25] and OpenAI [26] demonstrated that LLMs can extract high-level semantics from multimodal sensory inputs—such as vision, sonar, and inertial data—compressing noisy signals into structured representations that aid reasoning under uncertainty. Chen *et al*. [23] further showed that semantics enable meaning-centered, noise-resilient communication in underwater environments that preserves essential information under extreme compression. However, Fernandez *et al*. [28] noted that semantics alone lack interpretability for direct control, motivating the integration of LLM-based semantic reasoning with fuzzy inference, since fuzzy logic provides a transparent and stable mapping from semantics to control, enabling robots to achieve coherent, interpretable, and adaptive cooperation in uncertain underwater environments [32], [33].

C. Interpretable and Fuzzy Control for Robust Multi-Robot Systems

While semantic abstraction provides contextual awareness, effective multi-robot cooperation further depends on interpretable control mechanisms capable of translating high-level semantics into low-level actions. Zadeh [32] pioneered fuzzy logic as a means of "computing with words," enabling systems to handle linguistic uncertainty through continuous-valued reasoning. Building upon this foundation, Lu *et al*. [33] demonstrated that fuzzy systems remain highly effective for robust control under noisy or uncertain conditions. Fernandez *et al*. [28] summarized explainable fuzzy systems, emphasizing interpretability and human auditability—key features for safety-critical robotics. Besides, Zhang *et al*. [34] developed a leaderless adaptive fuzzy consensus control method for stochastic nonlinear multi-agent systems, where fuzzy reasoning and Nussbaum-type adaptation enhanced robustness against false data injection and sensor uncertainty, achieving distributed consensus with reduced communication overhead. These studies collectively highlight fuzzy control's unique strength in bridging symbolic reasoning and quantitative actuation, making it a natural complement to semantic or LLM-based perception modules.

In the context of cooperative robotics and multi-agent systems, hybrid frameworks integrating fuzzy reasoning with learning-based coordination have been proposed to balance local adaptability and global consistency. Yang *et al*. [35] developed an off-policy fuzzy RL approach for two time-scale nonlinear multi-agent systems, enabling adaptive local control and consistent global formation without full dynamic knowledge. In parallel, Yan *et al*. [36] designed an adaptive fuzzy RL control method for switched stochastic nonlinear systems with actuator faults, achieving fault tolerance and prescribed performance through an event-triggered actor–critic framework. More recently, Zhang *et al*. [37] presented a fuzzy RL method for prescribed-time optimal formation control of

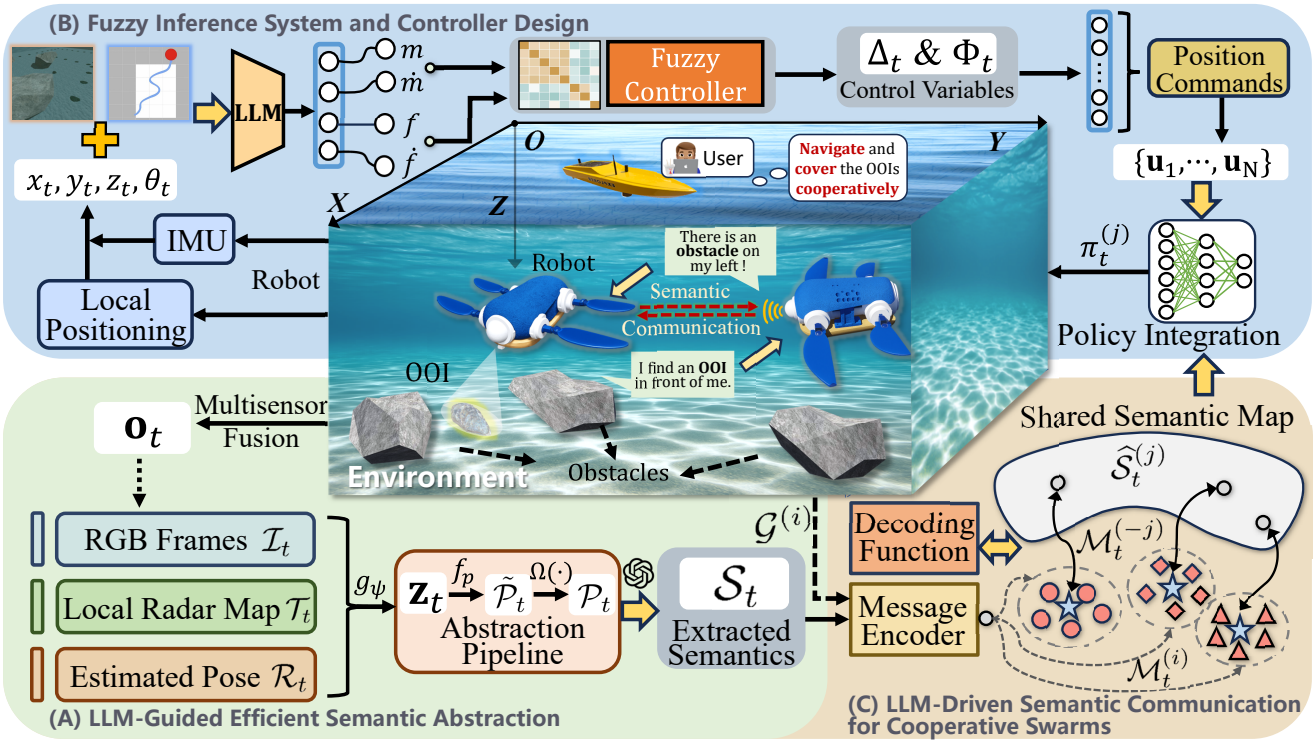

Fig. 2. **Overview of the semantics-guided fuzzy control framework**, which consists of three modules: (A) LLM-Guided Efficient Semantic Abstraction; (B) Fuzzy Inference System and Controller Design; (C) LLM-Driven Semantic Communication for Cooperative Swarms. The framework integrates LLM-guided semantic abstraction, fuzzy inference control, and semantic communication to form a closed-loop perception–reasoning–action cycle. Together, these modules enable interpretable, adaptive, and cooperative navigation for the multi-robot system under uncertain underwater conditions.

nonlinear multi-agent systems, ensuring accurate and energy-efficient coordination. Despite advances in RL and distributed consensus control, purely data-driven approaches often suffer from limited interpretability and adaptability in complex multi-agent scenarios [38]. Therefore, integrating fuzzy inference with LLM-derived semantic reasoning provides a promising path toward interpretable and adaptive swarm coordination, particularly for underwater robotic systems operating under uncertainty [39].

III. METHODOLOGY

In this section, we introduce the proposed framework in detail. Its overall architecture is depicted in Fig. 2, which comprises three modules. Together, these modules form a semantics-guided fuzzy control framework that ensures cooperative multi-robot underwater coverage.

A. LLM-Guided Efficient Semantic Abstraction

Effective underwater navigation and coverage require transforming high-volume, multimodal data into compact and interpretable representations. Traditional pipelines often transmit raw sensor inputs, such as RGB frames $\mathcal{I}_t$, local radar maps $\mathcal{R}_t$, and the robot's locally estimated pose $\mathcal{T}_t$, leading to redundancy and limited interpretability under bandwidth and sensing constraints [40]. To address this issue, our framework adopts an LLM-guided semantic abstraction paradigm, wherein raw sensory inputs $\mathbf{o}_t = \{\mathcal{I}_t, \mathcal{R}_t, \mathcal{T}_t\}$ are converted into $\mathcal{S}_t = \{s_1, s_2, \ldots, s_n\}$, which denote the concise and extracted semantic descriptors that encode environmental structure, obstacle distribution, and exploration potential. Mathematically, this abstraction can be expressed as a mapping:

$$\mathcal{F}_{\text{SA}} : \ \mathbf{o}_t \rightarrow \mathcal{S}_t, \tag{1}$$

where $\mathcal{F}_{\text{SA}}$ denotes the semantic abstraction function that bridges perception and decision-making, enabling downstream reasoning to operate on structured semantics rather than unprocessed measurements.

1) Multimodal Perception and Semantic Encoding: To support this abstraction process, each robot is equipped with an RGB camera, an Inertial Measurement Unit (IMU), and a local positioning module for environmental perception. At time step t, the robot's locally estimated pose is defined as $\mathcal{T}_t = (t, x_t, y_t, z_t, \theta_t)$, where $\mathbf{p}_t = (x_t, y_t, z_t)$ and θ_t denote the position and heading within the robot's local reference frame. To prevent redundant exploration and overlapping coverage among robots, a local radar map $\mathcal{R}_t$ is maintained in the form of an occupancy grid $\mathcal{O}_t \in \mathbb{R}^{W \times H}$, enabling each robot to reason about previously visited regions. This occupancy grid, with a spatial resolution r, is continuously updated as follows:

$$\mathcal{O}_t = \left\{ \left(\left\lfloor \frac{x_i}{r} \right\rfloor, \left\lfloor \frac{y_i}{r} \right\rfloor \right) \ \middle| \ i = 1, \ldots, t \right\}, \tag{2}$$

allowing each robot to maintain a lightweight yet dynamically evolving spatial memory of its surroundings. In practice, the local radar map $\mathcal{R}_t$ is projected onto the occupancy grid $\mathcal{O}_t$, which is incrementally updated to record the explored cells.

The fused multimodal observation vector $\mathbf{o}_t = [\mathcal{I}_t, \mathcal{R}_t, \mathcal{T}_t]$ is then processed by a perception encoder $g_\psi(\cdot)$ to obtain a latent representation $\mathbf{z}_t = g_\psi(\mathbf{o}_t) \in \mathbb{R}^m$, which captures essential spatial and contextual cues for subsequent reasoning. Building upon this latent encoding, an LLM-driven compression module $f_p(\cdot)$ generates a preliminary linguistic representation, referred to as a proto-prompt $\tilde{\mathcal{P}}_t = f_p(\mathbf{z}_t)$, which serves as an intermediate semantic interface between perception and language. Each proto-prompt $\tilde{\mathcal{P}}_t$ is composed of a set of linguistic tokens $\mathcal{L}_t = \{\ell_1, \ell_2, \ldots, \ell_d\}$, where each token ℓ_t represents a high-level natural-language description of the current environment—for example:

```
"Front area partially explored;
 dense obstacles on the left."
```

These tokens act as interpretable carriers of spatial and contextual knowledge, which are further refined into structured prompts for reasoning.

2) Structured Prompting for Context-Aware Semantic Reasoning: Building upon the proto-prompt $\tilde{\mathcal{P}}_t$, the next stage constructs a structured reasoning prompt $\mathcal{P}_t = \Omega(\tilde{\mathcal{P}}_t, \mathcal{I}_t, \mathcal{R}_t, \mathcal{T}_t)$ to guide the pretrained LLM $\mathcal{F}_{\text{LLM}}$ in generating context-aware and physically grounded semantics [41], [42]. The LLM then performs semantic reasoning as follows:

$$\mathcal{S}_t = \mathcal{F}_{\text{LLM}}(\mathcal{P}_t), \tag{3}$$

These extracted descriptors $\mathcal{S}_t$ serve as high-level semantic abstractions distilled from the linguistic token set $\mathcal{L}_t$, encapsulating the essential environmental and contextual information required for downstream reasoning and control. In this way, $\mathcal{S}_t$ bridges the gap between perception-level linguistic encoding and task-level decision-making, functioning as a compact yet expressive semantic abstract representation.

To guaranty that the extracted semantics $\mathcal{S}_t$ remain both physically meaningful and behaviorally consistent, each structured prompt $\mathcal{P}_t$ is generated under a set of semantic constraints that regulate environmental grounding, temporal continuity, and goal alignment:

- **Environmental grounding:** $\mathcal{S}_t \Leftarrow \phi_e(\mathcal{O}_t, \mathcal{I}_t)$, where $\phi_e(\cdot)$ extracts salient spatial cues from the occupancy grid $\mathcal{O}_t$ and RGB frames $\mathcal{I}_t$, ensuring that the resulting semantics remain consistent with the robot's physical and environmental surroundings;
- **Behavioral continuity:** $\mathcal{S}_t \approx \mathcal{S}_{t-1} + \Delta_t$, where $\Delta_t = \mathcal{S}_t - \mathcal{S}_{t-1}$ captures short-horizon evolutions of semantics, enforcing smooth temporal transitions and preventing abrupt shifts in reasoning or decision-making in motion;
- **Goal alignment:** $\mathcal{S}_t \models \mathcal{G}$, where $\mathcal{G}$ denotes the mission-level objective (e.g., maximizing area coverage or minimizing re-visitation), ensuring that semantic inference remains explicitly conditioned on high-level task goals.

Taken together, these constraints define the structured prompt generation process, ensuring that each semantic representation remains physically grounded, temporally consistent, and aligned with the mission objectives.

In summary, the overall semantic abstraction pipeline can be expressed as:

$$\mathbf{o}_t \xrightarrow{g_\psi} \mathbf{z}_t \xrightarrow{f_p} \tilde{\mathcal{P}}_t \xrightarrow{\Omega(\cdot)} \mathcal{P}_t \xrightarrow{\mathcal{F}_{\text{LLM}}} \mathcal{S}_t, \tag{4}$$

which represents a hierarchical transformation from raw multimodal perception $\mathbf{o}_t$ to the extracted semantic descriptors $\mathcal{S}_t$, which can be further expressed in compact form as:

$$\mathcal{F}_{\text{SA}} = \mathcal{F}_{\text{LLM}} \circ \Omega(\cdot) \circ f_p \circ g_\psi, \tag{5}$$

where $\mathcal{F}_{\text{SA}}$ encapsulates the semantic abstraction pipeline by integrating latent encoding, structured prompting, and LLM-based inference into a unified framework. Combining structured prompts with language-level reasoning, this process bridges unstructured perception and structured decision-making, enabling real-time adaptability, contextual awareness, and communication-efficient cooperation for underwater swarm coverage under degraded sensing conditions.

B. Fuzzy Inference System and Controller Design

Building upon the LLM-guided semantic abstraction, the extracted semantic descriptors $\mathcal{S}_t$ provide a compact and interpretable representation of the robot's situational awareness. To translate these high-level semantics into actionable control signals, a fuzzy inference system is developed to bridge symbolic reasoning and continuous motion control. Within this system, the pretrained LLM further refines $\mathcal{S}_t$ into a set of fuzzy linguistic variables that explicitly encode navigational intent—such as advancing toward regions dense with OOIs and avoiding redundant revisitation.

1) Fuzzy Inference System: To enable interpretable yet flexible control, these LLM-derived fuzzy variables are organized into four key dimensions that jointly describe the robot's motion tendencies: turning bias (`Moment`), its temporal rate of change (`MomentChange`), propulsion strength (`Force`), and its variation over time (`ForceChange`). Together, they form an intermediate semantic–control interface, providing structured and continuous-valued inputs for the fuzzy inference system to generate smooth actuation commands:

$$\ell_1 = \texttt{Moment} \in \{\texttt{NB}, \texttt{NM}, \texttt{ZO}, \texttt{PM}, \texttt{PB}\}, \tag{6a}$$
$$\ell_2 = \texttt{MomentChange} \in \{\texttt{NB}, \texttt{NM}, \texttt{ZO}, \texttt{PM}, \texttt{PB}\}, \tag{6b}$$
$$\ell_3 = \texttt{Force} \in \{\texttt{ZO}, \texttt{PS}, \texttt{PM}, \texttt{PB}\}, \tag{6c}$$
$$\ell_4 = \texttt{ForceChange} \in \{\texttt{NB}, \texttt{NM}, \texttt{ZO}, \texttt{PM}, \texttt{PB}\}. \tag{6d}$$

The above fuzzy label set is denoted as $\mathcal{Q} = \{q_1, q_2, q_3, q_4\}$, representing a compact and interpretable bridge between semantic reasoning and low-level actuation. Each linguistic variable is defined over a normalized universe of discourse corresponding to its operational range:

- Moment: [-0.2, 0.2], MomentChange: [-3, 3];
- Force: [0, 1], ForceChange: [-3, 3].

Through this semantic-to-fuzzy mapping, the high-level intent is grounded in continuous, physically meaningful variables that can be directly utilized for control. This mechanism not only ensures a smooth transition from symbolic reasoning to actuation, but also enhances adaptability, allowing the robot to generalize navigation and motion behaviors across uncertain environments without retraining.

TABLE I
FUZZY RULE TABLES FOR Δ AND Φ

m \ $\dot{m}$	NB	NM	ZO	PM	PB
NB	NB	NB	NM	ZO	ZO
NM	NB	NM	ZO	PM	PB
ZO	NM	ZO	ZO	ZO	PM
PM	ZO	PM	ZO	PM	PB
PB	ZO	PM	PM	PB	PB

f \ $\dot{f}$	NB	NM	ZO	PM	PB
ZO	ZO	ZO	ZO	PS	PM
PS	ZO	ZO	PS	PM	PM
PM	ZO	PS	PM	PM	PB
PB	PS	PM	PM	PB	PB

2) Fuzzy Controller Module: Building upon these fuzzy variables, the controller module translates linguistic intent into continuous control signals [43]. It defines four antecedent inputs—m (Moment), $\dot{m}$ (MomentChange), f (Force), and $\dot{f}$ (ForceChange)—which are mapped to two output variables representing the robot's steering and gait behaviors:

- $\Delta \in [-50,\ 50]$: angular steering adjustment;
- $\Phi \in [0,\ 1]$: normalized gait frequency.

Furthermore, expert-informed fuzzy rules encode high-level navigation strategies, while rich membership functions provide fine-grained control refinement across diverse underwater conditions. The corresponding rule sets are formally defined as:

$$\text{IF } m = A_i \text{ AND } \dot{m} = B_j \text{ THEN } \Delta = C_{ij}, \tag{7a}$$

$$\text{IF } f = D_k \text{ AND } \dot{f} = E_l \text{ THEN } \Phi = F_{kl}, \tag{7b}$$

where A_i, B_j, D_k, and E_l denote fuzzy linguistic terms corresponding to the robot's semantic descriptors. These rule tables embed human expert knowledge into the control process, ensuring that the generated actions remain smooth, interpretable, and stable under perceptual uncertainty and environmental variability.

To implement the expert-informed fuzzy rules, two lookup tables (Table I) are designed to encode navigation heuristics in an interpretable form. The first table computes the angular steering adjustment Δ from $(m, \dot{m})$, while the second derives the normalized gait frequency Φ from $(f, \dot{f})$. These rule bases embed expert knowledge directly into the control process, enabling smooth and adaptive actuation under perceptual uncertainty.

Then, the final control outputs are derived via centroid defuzzification:

$$\Delta = \frac{\int_{\mathbb{R}} \mu_\Delta(x) \cdot x\, dx}{\int_{\mathbb{R}} \mu_\Delta(x)\, dx}, \quad \Phi = \frac{\int_{\mathbb{R}} \mu_\Phi(x) \cdot x\, dx}{\int_{\mathbb{R}} \mu_\Phi(x)\, dx}, \tag{8}$$

where x represents the universe of discourse of the output variable (e.g., Δ or Φ), and $\mu_\Delta(x)$, $\mu_\Phi(x)$ denote the aggregated membership functions from fuzzy inference. This step transforms discrete linguistic reasoning into continuous and physically consistent control signals, enabling the robot to perform smooth and stable maneuvers during underwater navigation and coverage tasks.

Overall, the fuzzy controller serves as a semantic bridge between the LLM's symbolic intent and motor-level actuation, ensuring that high-level reasoning is faithfully translated into coherent, real-world motion behavior.

Algorithm 1 The Proposed Framework

Initialize all the three modules
Set initial position $\mathbf{p}_0$ and heading angle θ_0
Initialize gait phase index $\phi \leftarrow 0$
for each timestep $t = 0, 1, 2, \ldots$ **do**
  Capture RGB images $\mathcal{I}_t$ and local radar map $\mathcal{R}_t$
  Retrieve state: the robot's locally estimated pose $\mathcal{T}_t$
  if $\phi = 0$ **then**
    Extract semantic descriptors from $(\mathcal{I}_t, \mathcal{R}_t, \mathcal{T}_t)$
    Query LLM with prompt to obtain fuzzy labels:
      $\mathcal{Q}_t = \{q_1, q_2, q_3, q_4\}$
    Defuzzify outputs using fuzzy controller:
      $(\Delta_t, \Phi_t) \leftarrow \texttt{FuzzyController}(\mathcal{Q}_t)$
    Generate gait sequence based on Δ_t and Φ_t:
      $\mathcal{U}_t = \texttt{GenerateGait}(\Delta_t, \Phi_t)$
  end if
  Select and execute current motor command:
    $\mathbf{u}_t \leftarrow \mathcal{U}_t[\phi]$
    $\texttt{motor.setPosition}(\mathbf{u}_t[i]),\ i = 1, \ldots, 12$
  Update gait phase index:
    $\phi \leftarrow (\phi + 1) \bmod N$
end for

3) Modulated Gait Generation and Closed-Loop Execution: In the final stage, the robot executes motion control based on the generated control pair (Δ, Φ) which modulates its gait dynamics in a biologically interpretable manner. Specifically, the pair governs the gait system to produce a joint trajectory sequence $\mathcal{U} = \{\mathbf{u}_1, \ldots, \mathbf{u}_N\}$ over each gait cycle, where each vector $\mathbf{u}_i \in \mathbb{R}^{12}$ encodes 3-DOF position commands for the robot's four limbs. To achieve directional turning, an amplitude asymmetry is introduced between the left and right forelegs:

$$A_{\text{left}} = A_0 - \kappa \cdot \frac{\Delta}{\Delta_{\max}}, \quad A_{\text{right}} = A_0 + \kappa \cdot \frac{\Delta}{\Delta_{\max}}, \tag{9}$$

where A_0 is the base step amplitude, and κ scales the turning curvature. These parameters define the forward phase of the gait, with the hind legs following a synchronized, constant pattern. The joint commands are then applied to each motor, and their pseudo-code can be expressed as:

$$\texttt{motor.setPosition}(\mathbf{u}_t[i]), \quad i = 1, \ldots, 12. \tag{10}$$

In summary, the entire framework functions within a closed-loop architecture that continuously cycles through semantic reasoning, fuzzy control, and bio-inspired actuation. At the beginning of each gait cycle ($\phi_t = 0$), the LLM is queried to produce a new fuzzy label set $\mathcal{Q}_t$ based on the current visual input, the local radar map, and the robot's locally estimated pose. This label set is defuzzified into control variables (Δ_t, Φ_t) for the next steps, guiding the gait trajectory. The process is summarized as follows:

$$\mathcal{F}_{SA}(\mathcal{I}_t, \mathcal{R}_t, \mathcal{T}_t) \rightarrow \mathcal{Q}_t \rightarrow (\Delta_t, \Phi_t) \rightarrow \mathcal{U}_t \rightarrow \mathbf{u}_t. \tag{11}$$

This integrated loop (see pseudo-code in Algorithm 1) tightly couples semantic intention, perceptual understanding, and motor control, forming a cohesive perception–action cycle. Through this unified process, the robot can continuously

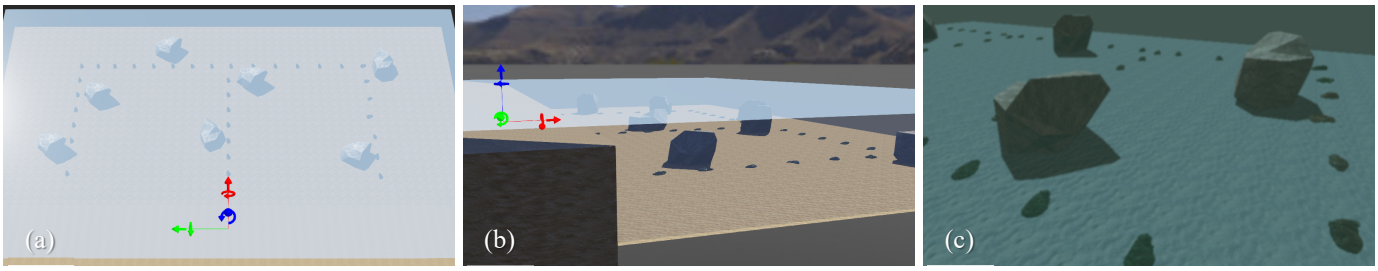

Fig. 3. Visualization of the underwater coverage task simulated in the Webots platform. (a) Top-down view. (b) Side view. (c) Robot's real-time camera feed.

interpret its environment, adjust its gait, and adapt its motion patterns for robust and autonomous navigation and coverage in complex underwater environments.

C. LLM-Driven Semantic Communication for Cooperative Swarms

Building upon the previously established framework, we further extend the approach to the multi-robot level to enable cooperative decision-making and information sharing. Specifically, we propose an LLM-driven semantic communication mechanism that allows robots to exchange compact, task-relevant, and human-interpretable information in linguistic form, enabling efficient and robust collaboration under limited connectivity and uncertain underwater conditions.

1) Semantic Encoding and Token Generation: At each communication round t_c, the i-th robot aggregates its local multimodal perception and reasoning outputs into a semantic intent message. Formally, given the local observation tuple $\mathbf{o}_t^{(i)} = \{\mathcal{I}_t^{(i)}, \mathcal{R}_t^{(i)}, \mathcal{T}_t^{(i)}\}$ and the corresponding LLM-inferred semantic abstract $\mathcal{S}_t^{(i)}$, the communication message is generated as follows:

$$\mathcal{M}_t^{(i)} = \mathcal{F}_{\text{LLM}}^{\text{enc}}\big(\mathcal{S}_t^{(i)}, \mathcal{G}^{(i)}\big), \tag{12}$$

where $\mathcal{F}_{\text{LLM}}^{\text{enc}}$ denotes a message encoder realized via structured prompting of the pretrained LLM, and $\mathcal{G}^{(i)}$ represents the robot's current sub-goal or task context. Each encoded message $\mathcal{M}_t^{(i)}$ consists of a set of semantic tokens:

$$\mathcal{M}_t^{(i)} = \{\tau_1^{(i)}, \tau_2^{(i)}, \ldots, \tau_d^{(i)}\}, \tag{13}$$

where each token $\tau_k^{(i)}$ corresponds to a distinct semantic element—such as local obstacle density, explored area direction, and heading intent—summarizing the robot's situational awareness in natural-language form (e.g., `"Right area clear, moving north toward unexplored region"`). The generated semantic tokens are transmitted through acoustic channels as concise linguistic representations, allowing robots to exchange high-level situational knowledge instead of raw sensory data.

2) Semantic Decoding and Cooperative Inference: Upon receiving messages from its peers, the j-th robot reconstructs a shared semantic map representing the swarm's collective understanding. This is achieved via an LLM-based decoding function $\mathcal{F}_{\text{LLM}}^{\text{dec}}$, which can be expressed as follows:

$$\widehat{\mathcal{S}}_t^{(j)} = \mathcal{F}_{\text{LLM}}^{\text{dec}}\big(\mathcal{M}_t^{(-j)}\big), \tag{14}$$

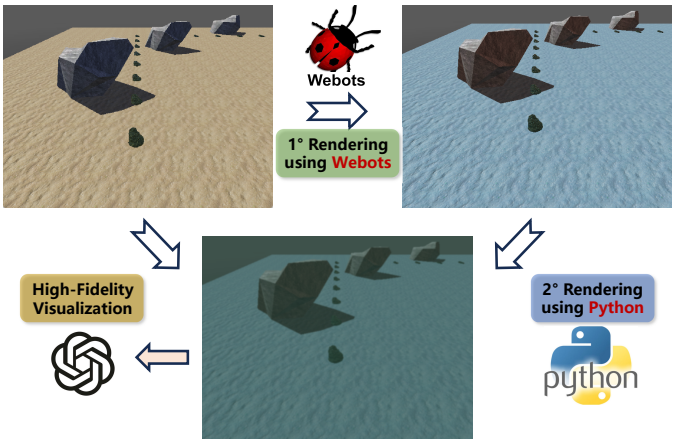

Fig. 4. Illustration of the two-stage rendering process, where the simulation scenes are first generated in Webots and subsequently refined in Python to produce a high-fidelity visualization.

where $\mathcal{M}_t^{(-j)}$ denotes the messages received from all other robots. The decoding process leverages contextual prompting to infer the swarm-level intent and align local actions accordingly:

$$\pi_t^{(j)} = \Pi\big(\mathcal{S}_t^{(j)}, \widehat{\mathcal{S}}_t^{(j)}\big), \tag{15}$$

where $\Pi(\cdot)$ denotes a policy integration module that merges the robot's local semantic abstract $\mathcal{S}_t^{(j)}$ with the shared semantic map $\widehat{\mathcal{S}}_t^{(j)}$. This allows each robot to dynamically adjust its navigation strategy—distributing coverage responsibilities, avoiding redundant coverage, or assisting peers in OOI-dense regions. Overall, the proposed framework enables the multi-robot system to share compact, interpretable intent information in linguistic form, establishing a distributed cognitive network that unifies perception, reasoning, and communication for adaptive cooperation in uncertain underwater environments.

IV. Experiments and Analysis

In this section, we begin with an introduction to the Webots-based simulation environment employed in this study, followed by a detailed presentation and analysis of the comprehensive experimental results.

A. Task Description and Experimental Settings

In this study, the proposed framework was evaluated through extensive simulations conducted on the Webots platform [44]. As illustrated in Fig. 3, the multi-robot system was deployed

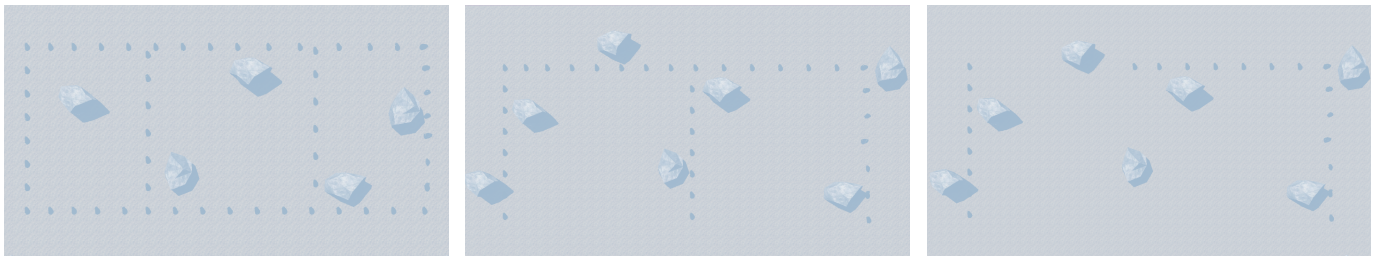

(a) Grid World (b) E-Shape (c) Disconnected Paths

Fig. 5. Top-view visualization of the three simulated underwater environments—Grid World, E-Shape, and Disconnected Paths, which are used to evaluate coverage performance under different spatial structures. (a) Grid World. (b) E-Shape. (c) Disconnected Paths.

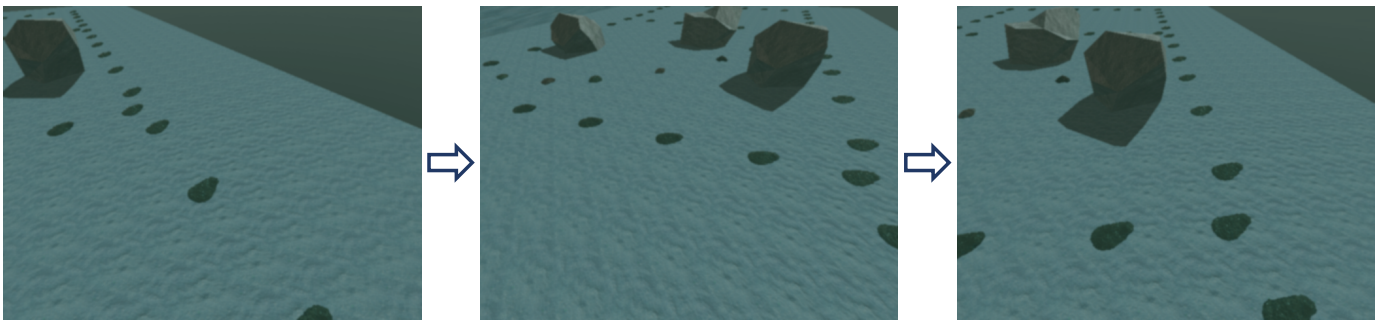

(a) Timestamp = 280 (b) Timestamp = 320 (c) Timestamp = 360

Fig. 6. Sequential snapshots showing the robot's forward navigation process across timestamps 280–360, demonstrating perception and continuous movement towards OOI-dense areas, while effectively avoiding obstacles in the simulated underwater environment. (a) Timestamp = 280. (b) Timestamp = 320. (c) Timestamp = 360.

TABLE II
KEY PARAMETERS OF THE EXPERIMENTAL SETUP.

Parameter	Value & Description
Number of robots	1 / 2 (default) / 3
Size of the experimental site	12 m × 8 m
Number of obstacles	5 / 7 / 7
Time step	256 ms
LLM model	GPT-4o
LLM parameters	temperature=0.1, Max tokens=300
LLM query frequency	every 4 frames
Camera resolution	640 × 480
Field of view	1.5 rad
Robot's dimensions	0.43 × 1.23 × 0.17 m³
Robot's weight	10.48 kg
Actuation Mechanism	12 servo motors, 3-DOF flippers
Sensing Modules	Camera, IMU, Radar-style sensor

to perform coverage missions over regions containing multiple OOIs under uncertain and partially observable conditions [31]. The robots were not provided with any global positioning information and instead relied solely on local observation and pose estimation for navigation, which closely mirrors the constraints of real-world underwater environments. To ensure smooth operation when the OOIs temporarily disappear from the camera view, each robot performed an in-place rotation until the OOIs reappeared, then proceeded in the direction where the OOIs were densest. To further narrow the sim-to-real discrepancy, input visual data were rendered following the procedure of prior work [45], as depicted in Fig. 4, while individual OOIs were instantiated using the oyster model introduced in [46].

When designing the simulation scenarios, we drew inspiration from the spatial organization of natural underwater reefs, particularly oyster formations that serve as our primary OOIs. Such reefs generally appear in large, clustered aggregations rather than as isolated colonies, though environmental factors often lead to discontinuous and fragmented patches. To reflect these ecological characteristics, three representative scenarios were developed:

- Grid World — a reef composed of interconnected oyster patches with multiple branching structures (Fig. 5(a));
- E-Shape — a wide C-shaped oyster reef featuring a narrow central patch (Fig. 5(b));
- Disconnected Paths — a reef consisting of two major oyster clusters separated by an extended sandy gap (Fig. 5(c)).

Such a configuration captures realistic challenges typical of ecological monitoring and environmental surveying tasks, where efficient spatial coverage is critical [47]. All key parameters used in the simulation are summarized in Table II.

For benchmarking, two classical coverage strategies—(1) Boustrophedon Cell Decomposition (BCD) [48] and (2) Brownian Bridge (BB) [49]—were implemented for comparison, as both are widely regarded as canonical methods in complete coverage path planning [50], [51]. Across all experiments, the robot was required to explore unstructured environments, avoid obstacles, and maximize OOI coverage while minimizing redundant traversal.

To rigorously quantify navigation and control performance,

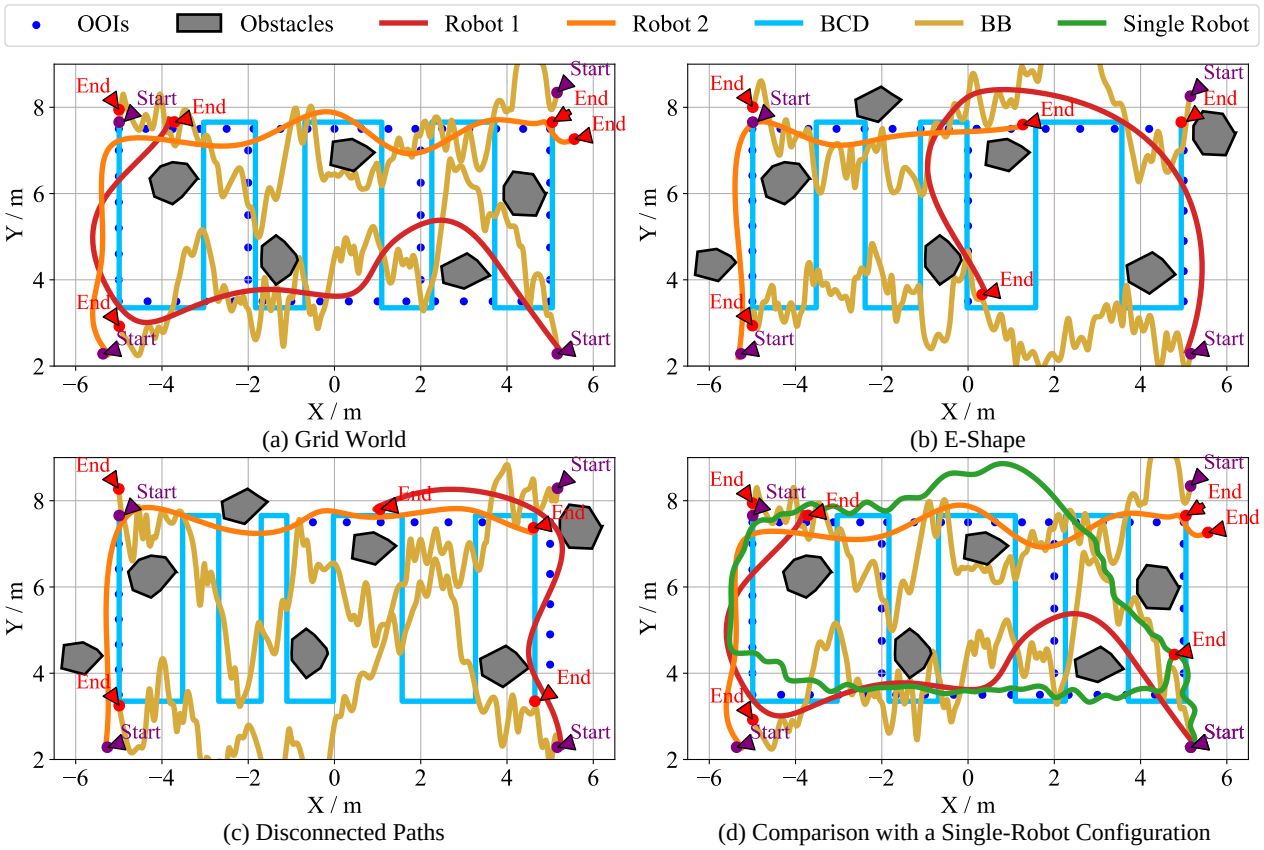

Fig. 7. Comparison of coverage trajectories generated by the two robots using the proposed framework and baseline methods (BCD, BB) across three different environments—Grid World, E-Shape, and Disconnected Paths, demonstrating effective obstacle avoidance and cooperative coverage performance. In addition, the trajectories of the two-robot configuration are compared with those of the single-robot setup in the Grid World environment for further analysis. (a) Grid World. (b) E-Shape. (c) Disconnected Paths. (d) Comparison with a Single-Robot Configuration.

three basic statistics were first collected: (1) the total length, defined as the overall trajectory distance; (2) the covered OOI number, representing all OOIs detected within a 0.7 m radius of the path; and (3) the coverage length, corresponding to the cumulative trajectory within OOI-dense areas. Based on these quantities, three normalized indicators were derived to provide a holistic evaluation of the proposed framework:

- **Coverage Ratio**: the proportion of OOI-rich regions successfully covered by the robot;
- **OOI Density**: the number of covered OOIs per meter of total path length;
- **OOI Efficiency**: the number of covered OOIs per meter of coverage length.

B. Experiment Results and Analysis

To evaluate the perceptual robustness of the proposed framework, we first conducted a simulation experiment in which two robots performed a coverage mission in a partially observable underwater environment. As shown in Fig. 6, the experiment records a robot's real-time visual perception at three representative timestamps (280, 320, and 360), illustrating how its onboard sensing evolves during navigation. The simulated scene contains multiple OOIs—modeled as clustered oyster reefs—and irregular obstacles. Without access to global positioning, the robot relied solely on local observation and pose estimation to navigate and complete coverage tasks. As time progressed, the distribution and scale of the OOI regions changed dynamically, revealing that the robot gradually approached and traversed OOI-dense areas while effectively avoiding obstacles. These results visually demonstrate the feasibility of LLM-guided semantic abstraction and fuzzy-control mechanisms, which together enable continuous environmental understanding and stable coverage behavior under degraded underwater visibility conditions.

We further evaluate the cooperative navigation and coverage performance of the proposed framework in complex underwater environments. As illustrated in Fig. 7, the trajectories show the results of different approaches, as well as a comparison between two-robot and single-robot configurations. In Fig. 7(a)-(c), blue dots denote OOIs, gray polygons represent obstacles, and the red and orange curves correspond to the trajectories of Robot 1 and Robot 2, respectively. The cyan and yellow curves indicate the classical baselines, BCD and BB. The system of two robots generates smooth and approximately non-redundant coverage paths that closely follow OOI-dense regions while effectively avoiding obstacles. In contrast, BCD exhibits rigid, grid-like sweeping patterns with limited semantic adaptability, whereas BB produces irregular, random movements with redundant coverage. In the E-Shape and Dis-

TABLE III
QUANTITATIVE COMPARISON OF THE PROPOSED FRAMEWORK AND BASELINE METHODS ACROSS THREE DIFFERENT ENVIRONMENTS.

Environment	Method	Coverage Ratio (%)	OOI Density (/m)	OOI Efficiency (/m cov)
Grid World	**Two Robots**	**69.52**	**1.25**	**1.79**
	Robot 1	77.58	1.35	1.74
	Robot 2	90.13	1.68	1.86
	Single Robot	75.29	1.20	1.59
	BCD	74.33	1.17	1.57
	BB	36.41	0.52	1.44
E-Shape	**Two Robots**	**73.84**	**1.30**	**1.77**
	Robot 1	67.43	1.21	1.79
	Robot 2	91.77	1.68	1.83
	Single Robot	82.41	1.32	1.61
	BCD	50.66	0.79	1.56
	BB	40.65	0.45	1.12
Disconnected Paths	**Two Robots**	**61.28**	**0.87**	**1.42**
	Robot 1	72.92	1.10	1.51
	Robot 2	68.22	1.05	1.54
	Single Robot	64.18	0.89	1.38
	BCD	32.51	0.43	1.34
	BB	13.91	0.18	1.30

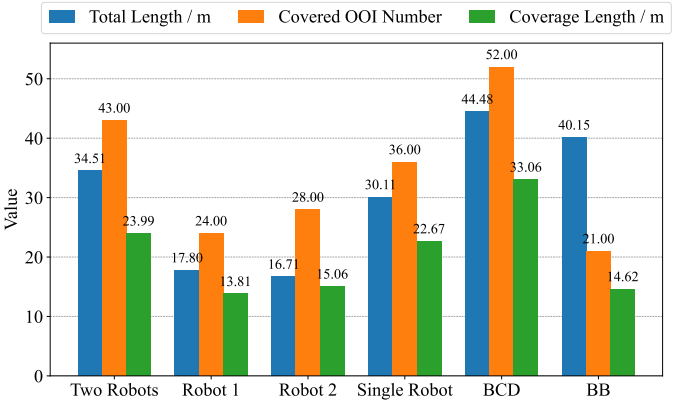

Fig. 8. Performance comparison in the Grid World environment, showing the total trajectory length, covered OOI Number, and effective coverage length achieved by different configurations and baseline methods.

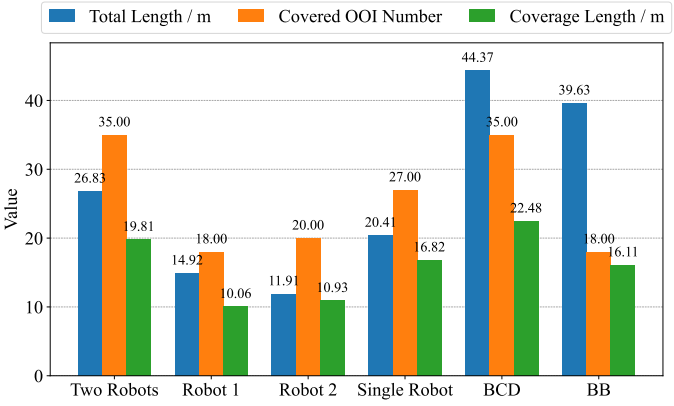

Fig. 9. Performance comparison in the E-Shape environment, showing the total trajectory length, covered OOI Number, and effective coverage length achieved by different configurations and baseline methods.

connected Paths scenarios, the two robots adaptively partition the workspace, minimizing cross-region traversal and overlap. The single-robot comparison in Fig. 7(d) further demonstrates

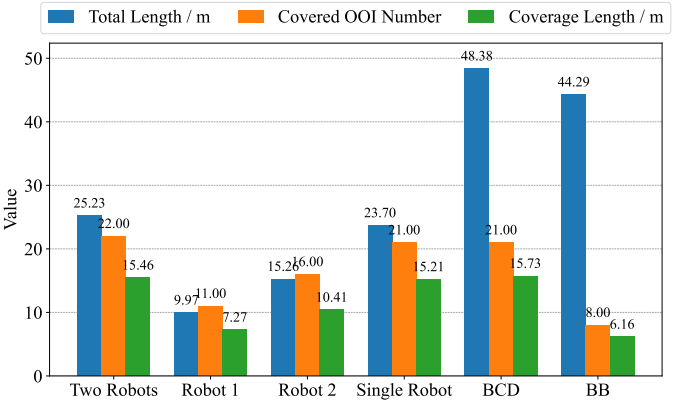

Fig. 10. Performance comparison in the Disconnected Paths environment, showing the total trajectory length, covered OOI Number, and effective coverage length achieved by different configurations and baseline methods.

that, under identical perceptual constraints, multi-robot cooperation significantly enhances coverage completeness and efficiency. Overall, these experiments validate that the LLM-guided fuzzy-control framework enables coordinated, robust, and efficient multi-robot adaptive coverage in spatially discontinuous and uncertain underwater environments.

To quantitatively evaluate the proposed framework, three statistical metrics—Total Length, Covered OOI Number, and Coverage Length—were collected for each environment, as shown in Figs. 8–10. These indicators correspond respectively to the overall trajectory distance, the number of OOIs detected within the coverage radius, and the cumulative trajectory length traversing OOI-dense regions. Across all scenarios, the Two Robots configuration consistently achieved a favorable balance between trajectory efficiency and coverage performance. In the Grid World environment (Fig. 8), it detected 43 OOIs with a total length of 34.51 m, achieving a more compact and efficient coverage trajectory compared with BCD (44.48 m, 52 OOIs) and BB (40.15 m, 21 OOIs). While BCD covered slightly more OOIs, the proposed framework

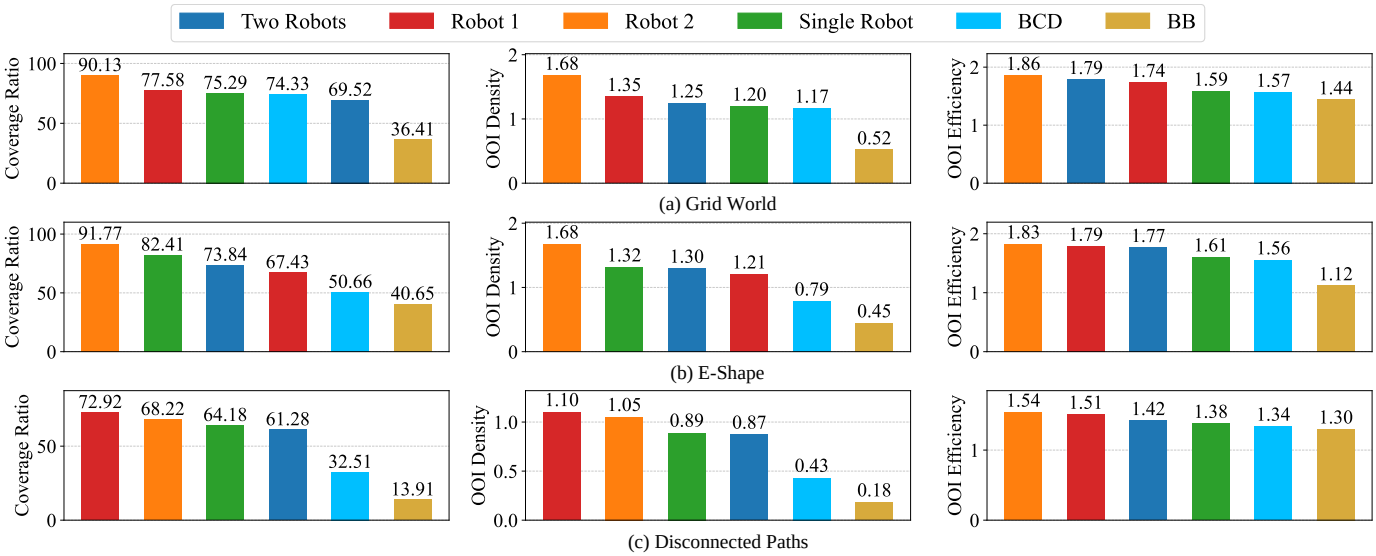

Fig. 11. Quantitative comparison of the proposed framework and baseline methods (BCD, BB) across three different environments—Grid World, E-Shape, and Disconnected Paths—in terms of coverage ratio, OOI density, and OOI efficiency, demonstrating the advantages of the two-robot configuration. (a) Grid World. (b) E-Shape. (c) Disconnected Paths.

demonstrated better path economy and spatial focus. Compared with the Single Robot configuration (30.11 m, 36 OOIs), the Two Robots setup achieved higher overall coverage with a modest increase in trajectory length, reflecting improved task division and reduced redundancy between agents. In the E-Shape scenario (Fig. 9), the proposed framework maintained similar advantages, reaching 35 OOIs with only 26.83 m of travel, while both BCD and BB exhibited significantly longer trajectories (44.37 m and 39.63 m, respectively). Relative to the Single Robot case (20.41 m, 27 OOIs), the Two Robots configuration achieved a broader spatial reach and better utilization of trajectory segments across disconnected OOI clusters. Finally, in the Disconnected Paths case (Fig. 10), the Two Robots setup achieved 22 OOIs within a 25.23 m trajectory—nearly 40% shorter than BCD (48.38 m) and BB (44.29 m)—demonstrating its ability to adapt to fragmented spatial layouts while maintaining effective OOI coverage. The comparison with the Single Robot configuration (23.70 m, 21 OOIs) further indicates that cooperative deployment enhances coverage completeness without increasing motion costs. These experimental results are consistent with the quantitative indicators summarized in Table III, further confirming that the proposed LLM-guided fuzzy-control framework enables efficient, stable, and spatially adaptive multi-robot coverage under limited perception and communication in uncertain underwater environments.

To facilitate a more comprehensive and in-depth analysis, the proposed framework was further evaluated quantitatively using three key metrics—Coverage Ratio, OOI Density, and OOI Efficiency—across three representative underwater environments: Grid World, E-Shape, and Disconnected Paths. As summarized in Table III and visualized in Fig. 11, the proposed Two Robots configuration consistently achieves superior overall performance compared with the classical BCD and BB baselines, while maintaining comparable efficiency to the Single Robot setup. In the Grid World scenario, the two-robot system attains a coverage ratio of 69.52% and an OOI density of 1.25 m^{-1}, outperforming BCD (74.33%, 1.17 m^{-1}) and BB (36.41%, 0.52 m^{-1}) through shorter and more focused trajectories. Although the Single Robot configuration achieves a slightly higher coverage ratio (75.29%), it requires longer traversal and shows less cooperative efficiency compared to the distributed Two Robots setup. It is worth noting that, even though the absolute coverage metrics of the Two Robots configuration are not the highest, the simultaneous exploration conducted by two agents effectively doubles the overall system's coverage efficiency within the same time frame. In the E-Shape environment, characterized by narrow passages and partially occluded OOI clusters, the proposed system sustains strong performance (73.84%, 1.30 m^{-1}), significantly surpassing BCD (50.66%, 0.79 m^{-1}) and BB (40.65%, 0.45 m^{-1}). Notably, Robot 2 individually attains the highest coverage ratio (91.77%) and density (1.68 m^{-1}), demonstrating the adaptability of the proposed framework in constrained and elongated reef structures. Here as well, although the overall coverage ratio of the two-robot system is slightly lower than that of the best-performing single agent, its parallel execution leads to nearly twice the effective exploration throughput, which is particularly beneficial for time-sensitive underwater operations. In the Disconnected Paths environment—where OOIs are spatially separated into distinct regions—the two-robot system maintains robust coverage (61.28%, 0.87 m^{-1}) and efficiency (1.42 m^{-1}), outperforming BCD (32.51%, 0.43 m^{-1}) and BB (13.91%, 0.18 m^{-1}), while achieving comparable coverage to the Single Robot case (64.18%) with reduced overlap and improved path distribution. Given that both robots operate concurrently in disjoint subregions, the overall spatial exploration efficiency is nearly doubled, confirming the scalability and cooperative potential of the proposed design. Although BCD occasionally exhibits slightly

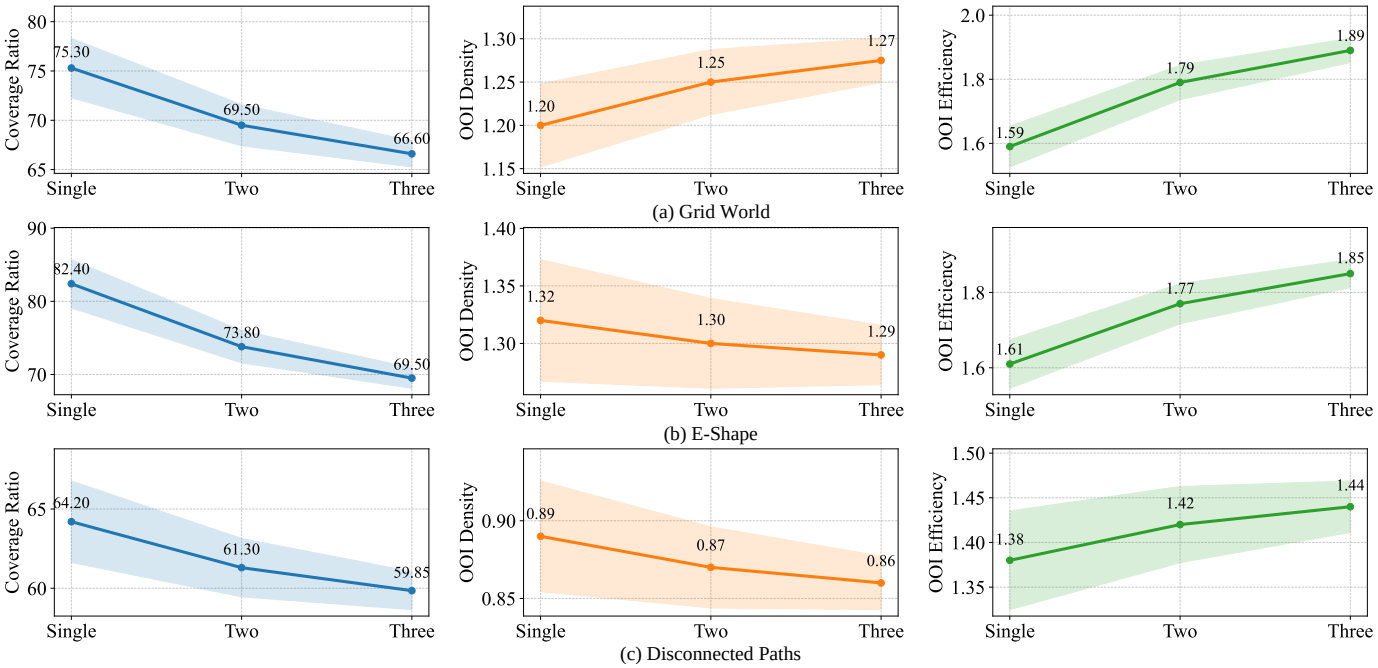

Fig. 12. Performance trends of the proposed framework in three environments—Grid World, E-Shape, and Disconnected Paths—showing how coverage ratio, OOI density, and OOI efficiency evolve as the number of robots increases from one to three. (a) Grid World. (b) E-Shape. (c) Disconnected Paths.

higher OOI efficiency values (e.g., 1.57 in Grid World), this stems from its rigid sweeping behavior rather than adaptive control or semantic coordination, leading to suboptimal coverage in fragmented environments. Collectively, these results indicate that the proposed LLM-guided fuzzy-control framework achieves a superior trade-off between global coverage and local efficiency across varying terrain types—from continuous to discontinuous OOI distributions. The Two Robots configuration demonstrates strong scalability, stable cooperation, and efficient path utilization. Despite not always attaining the absolute best coverage numbers, its parallel multi-agent operation effectively doubles exploration efficiency, making it highly suitable for cooperative underwater coverage under limited perception, partial observability, and communication constraints.

Following the quantitative comparison presented in Table III, Fig. 12 further illustrates the evolutionary trends of the three key performance metrics—Coverage Ratio, OOI Density, and OOI Efficiency—as the number of robots increases from single to dual and triple configurations across three representative environments: Grid World, E-Shape, and Disconnected Paths. This visualization complements the tabulated data by revealing how cooperative scale affects both global coverage and local exploration efficiency under limited perception and communication. As shown in Fig. 12, the coverage ratio exhibits a gradual decline when transitioning from a single- to a two-robot configuration (e.g., 75.30 $\rightarrow$ 69.50 in Grid World; 82.40 $\rightarrow$ 73.80 in E-Shape), and further to three robots (66.60 and 69.50, respectively). This decrease is primarily due to geometric segmentation and task overlap during parallel exploration. Meanwhile, the OOI density shows a slight improvement in Grid World (1.20 $\rightarrow$ 1.25 $\rightarrow$ 1.27) and remains nearly stable in E-Shape (1.32 $\rightarrow$ 1.30 $\rightarrow$ 1.29) and Disconnected Paths (0.89 $\rightarrow$ 0.87 $\rightarrow$ 0.86). In contrast, the OOI efficiency increases steadily across all environments (e.g., 1.59 $\rightarrow$ 1.79 $\rightarrow$ 1.89 in Grid World; 1.61 $\rightarrow$ 1.77 $\rightarrow$ 1.85 in E-Shape), reflecting a continuous improvement in the rate of effective OOI discovery per unit of coverage length. In the Disconnected Paths environment, where OOI clusters are spatially separated, the two-robot configuration achieves a coverage ratio (61.30%) comparable to the single-robot case (64.20%) but completes the task with improved efficiency (1.38 $\rightarrow$ 1.42), while the three-robot setup maintains similar overall performance with reduced variance. Although the absolute coverage ratios of multi-robot configurations are slightly lower, it is important to note that the system performs simultaneous exploration across multiple regions, effectively doubling or tripling the spatial throughput within the same operational timeframe. The shaded regions extending toward the three-robot configuration indicate a potential convergence in performance variance, suggesting that larger teams can improve overall stability and reduce individual fluctuation. Taken together, these observations reinforce the paper's broader conclusion: under weak global localization and partially observable conditions, increasing the number of cooperating robots primarily enhances local efficiency and temporal throughput, whereas improvements in global coverage remain constrained by geometric partitioning and coordination overhead—highlighting the need for further optimization through semantic task allocation and redundancy-aware coordination strategies.

V. Conclusion

This paper presents a semantics-guided fuzzy control framework that couples LLM-based semantic abstraction, an interpretable fuzzy inference and control module, and lightweight semantic communication to enable cooperative underwater

coverage with a multi-robot system. By compressing raw multimodal observations into compact, human-readable tokens and translating them into smooth steering and gait commands, the framework bridges perception, reasoning, and actuation under partial observability and communication constraints. Comprehensive Webots-based simulations across three representative environments demonstrated that the multi-robot system consistently achieves a superior trade-off between global coverage and local efficiency compared with classical BCD and BB baselines, while remaining competitive with a single-robot setup in terms of path economy and robustness. The system further exhibited stable coordination, reduced redundancy, and adaptability to spatial discontinuities; extrapolations toward three-robot teams suggest improved stability with diminishing returns in coverage, highlighting the importance of coordinated role assignment.

Despite these gains, several limitations remain. The current study relies on simulation with high-fidelity rendering; real-world trials are needed to assess acoustic/optic degradation, flow disturbances, and localization drift. The LLM component, while powerful, introduces prompt sensitivity and computational overhead; robustness to distribution shifts and energy-aware on-board deployment warrant further investigation. Communication was modeled as concise semantic tokens; however, scheduling under stringent acoustic latency/bandwidth, packet loss, and adversarial noise requires deeper treatment. Finally, coverage improvements are partly bounded by geometric segmentation and the residual overlap between agents.

Future work will extend the proposed framework from simulation to real-world deployment while addressing the key challenges identified above. A primary focus will be on semantics-aware task allocation and redundancy-aware planning to better exploit larger robot teams and mitigate geometric segmentation or trajectory overlap. In parallel, reliability-adaptive semantic communication integrating rate control, error correction, and intent-level consensus will be explored to maintain cooperation under acoustic latency, bandwidth limitations, and packet loss. To enhance scalability, future studies will examine on-robot LLM compression, distillation, and self-supervised grounding to reduce prompt sensitivity, computation, and energy consumption during inference. Finally, closed-loop field experiments with multimodal sensing (sonar, optics, and INS) and hydrodynamic modeling will be conducted to validate robustness under perception degradation and localization drift. Overall, integrating semantic cognition with fuzzy control establishes a scalable foundation for interpretable and cooperative underwater coverage in partially observable environments.

VI. Acknowledgment

This paper presents a semantics-guided fuzzy control framework that focuses on multi-robot underwater navigation and coverage under limited perception and communication. Although the primary contribution lies in the control and coordination methodology, the simulation experiments were conducted using a customized bio-inspired turtle robot model. The design of this model was inspired by the original robotic turtle prototype reported in a recent paper from Prof. Juntian Qu's group at Tsinghua University, based on which we developed our own modified version to achieve higher visual fidelity and a more realistic underwater simulation. We sincerely appreciate Prof. Juntian Qu and his students Ang Liu and Xianrui Zhang for their inspiring work and contributions to the original design.

References

[1] Z. Zhou, J. Liu, and J. Yu, "A survey of underwater multi-robot systems," *IEEE/CAA Journal of Automatica Sinica*, vol. 9, no. 1, pp. 1–18, 2022.

[2] Y. Yang, Y. Xiao, and T. Li, "A survey of autonomous underwater vehicle formation: Performance, formation control, and communication capability," *IEEE Communications Surveys & Tutorials*, vol. 23, no. 2, pp. 815–841, 2021.

[3] Z. Chu, Y. Wang, and D. Zhu, "Local 2-d path planning of unmanned underwater vehicles in continuous action space based on the twin-delayed deep deterministic policy gradient," *IEEE Transactions on Systems, Man, and Cybernetics: Systems*, vol. 54, no. 5, pp. 2775–2785, 2024.

[4] Y. Yang, Y. Xiao, and T. Li, "A survey of autonomous underwater vehicle formation: Performance, formation control, and communication capability," *IEEE Communications Surveys & Tutorials*, vol. 23, no. 2, pp. 815–841, 2021.

[5] Z. Zeng, S. Fu, H. Zhang, Y. Dong, and J. Cheng, "A survey of underwater optical wireless communications," *IEEE Communications Surveys & Tutorials*, vol. 19, no. 1, pp. 204–238, 2017.

[6] J. S. Jaffe, "Underwater optical imaging: The past, the present, and the prospects," *IEEE Journal of Oceanic Engineering*, vol. 40, no. 3, pp. 683–700, 2015.

[7] B. Li, S. Zhou, M. Stojanovic, L. Freitag, and P. Willett, "Multicarrier communication over underwater acoustic channels with nonuniform doppler shifts," *IEEE Journal of Oceanic Engineering*, vol. 33, no. 2, pp. 198–209, 2008.

[8] L. Huang, Y. Wang, Q. Zhang, J. Han, W. Tan, and Z. Tian, "Machine learning for underwater acoustic communications," *IEEE Wireless Communications*, vol. 29, no. 3, pp. 102–108, 2022.

[9] O. Ozkahraman and P. Ogren, "Combining control barrier functions and behavior trees for multi-agent underwater coverage missions," in *2020 59th IEEE Conference on Decision and Control (CDC)*, 2020, pp. 5275–5282.

[10] S. B. Gibson and D. J. Stilwell, "Hydrodynamic parameter estimation for autonomous underwater vehicles," *IEEE Journal of Oceanic Engineering*, vol. 45, no. 2, pp. 385–394, 2020.

[11] C. Lin, Y. Zhang, G. Han, C. Lu, S. Zhu, and S. Wang, "Multiple autonomous underwater vehicles-assisted data collection in 6g-driven underwater wireless networks based on software-defined marl," *IEEE Transactions on Intelligent Transportation Systems*, pp. 1–12, 2025.

[12] Y. Cao, W. Yu, W. Ren, and G. Chen, "An overview of recent progress in the study of distributed multi-agent coordination," *IEEE Transactions on Industrial Informatics*, vol. 9, no. 1, pp. 427–438, 2013.

[13] Y. Liu, M. Peng, G. Shou, Y. Chen, and S. Chen, "Toward edge intelligence: Multiaccess edge computing for 5g and internet of things," *IEEE Internet of Things Journal*, vol. 7, no. 8, pp. 6722–6747, 2020.

[14] E. Galceran and M. Carreras, "A survey on coverage path planning for robotics," *Robot. Auton. Syst.*, vol. 61, no. 12, p. 1258–1276, Dec. 2013.

[15] C. Ma, H. Zou, and X. An, "A complete coverage path planning approach for an autonomous underwater helicopter in unknown environment based on vfh+ algorithm," *Journal of Marine Science and Engineering*, vol. 12, no. 3, 2024.

[16] W. Ren and R. Beard, "Consensus seeking in multiagent systems under dynamically changing interaction topologies," *IEEE Transactions on Automatic Control*, vol. 50, no. 5, pp. 655–661, 2005.

[17] T. T. Nguyen, N. D. Nguyen, and S. Nahavandi, "Deep reinforcement learning for multiagent systems: A review of challenges, solutions, and applications," *IEEE Transactions on Cybernetics*, vol. 50, no. 9, pp. 3826–3839, 2020.

[18] K. Arulkumaran, M. P. Deisenroth, M. Brundage, and A. A. Bharath, "Deep reinforcement learning: A brief survey," *IEEE Signal Processing Magazine*, vol. 34, no. 6, pp. 26–38, 2017.

[19] E. Sebastián, T. Duong, N. Atanasov, E. Montijano, and C. Sagüés, "Physics-informed multiagent reinforcement learning for distributed multirobot problems," *IEEE Transactions on Robotics*, vol. 41, pp. 4499–4517, 2025.
[20] Z. Zhu, K. Lin, A. K. Jain, and J. Zhou, "Transfer learning in deep reinforcement learning: A survey," *IEEE Transactions on Pattern Analysis and Machine Intelligence*, vol. 45, no. 11, pp. 13 344–13 362, 2023.
[21] G. Y. Li, Y. C. Eldar, A. Behboodi, and G. Liu, "Guest editorial: Semantic communications: Transmission beyond shannon," *IEEE Communications Magazine*, vol. 61, no. 11, pp. 34–35, 2023.
[22] C. Zhang, L. Huang, and Q. Ning, "Resource allocation in wireless semantic communications: A comprehensive survey," *IEEE Communications Surveys & Tutorials*, pp. 1–1, 2025.
[23] W. Chen, W. Xu, H. Chen, X. Zhang, Z. Qin, Y. Zhang, and Z. Han, "Semantic communication based on large language model for underwater image transmission," *IEEE Transactions on Mobile Computing*, pp. 1–15, 2025.
[24] Y. Peng, J. Liu, Y. Zhu, R. Zhang, and F. Yuan, "Efficient semantic communication for underwater images guided by physical priors," *IEEE Signal Processing Letters*, vol. 32, pp. 3072–3076, 2025.
[25] D. W. Otter, J. R. Medina, and J. K. Kalita, "A survey of the usages of deep learning for natural language processing," *IEEE Transactions on Neural Networks and Learning Systems*, vol. 32, no. 2, pp. 604–624, 2021.
[26] D. Yang, E. Kleinman, and C. Harteveld, "Gpt for games: An updated scoping review (2020-2024)," *IEEE Transactions on Games*, pp. 1–16, 2025.
[27] H. Zhi, P. Chen, J. Li, S. Ma, X. Sun, T. Xiang, Y. Lei, M. Tan, and C. Gan, "Lscenellm: Enhancing large 3d scene understanding using adaptive visual preferences," in *2025 IEEE/CVF Conference on Computer Vision and Pattern Recognition (CVPR)*, 2025, pp. 3761–3771.
[28] A. Fernandez, F. Herrera, O. Cordon, M. Jose del Jesus, and F. Marcelloni, "Evolutionary fuzzy systems for explainable artificial intelligence: Why, when, what for, and where to?" *IEEE Computational Intelligence Magazine*, vol. 14, no. 1, pp. 69–81, 2019.
[29] R. Fu, J. Liu, X. Chen, Y. Nie, and W. Xiong, "Scene-llm: Extending language model for 3d visual reasoning," in *2025 IEEE/CVF Winter Conference on Applications of Computer Vision (WACV)*, 2025, pp. 2195–2206.
[30] H. Xing, S. Guo, L. Shi, X. Hou, Y. Liu, H. Liu, Y. Hu, D. Xia, and Z. Li, "A novel small-scale turtle-inspired amphibious spherical robot," in *2019 IEEE/RSJ International Conference on Intelligent Robots and Systems (IROS)*, 2019, pp. 1702–1707.
[31] A. Liu, X. Zhang, H. Huang, F. Xiao, Z. Zhang, G. Cui, B. Mao, Y. Xu, and J. Qu, "An intelligent bionic amphibious turtle robot with visual-tactile fusion for dynamic terrain adaptation," *IEEE Transactions on Robotics*, pp. 1–19, 2025.
[32] L. Zadeh, "Fuzzy logic = computing with words," *IEEE Transactions on Fuzzy Systems*, vol. 4, no. 2, pp. 103–111, 1996.
[33] J. Lu, G. Ma, and G. Zhang, "Fuzzy machine learning: A comprehensive framework and systematic review," *IEEE Transactions on Fuzzy Systems*, vol. 32, no. 7, pp. 3861–3878, 2024.
[34] H. Zhang, X. Guo, J. Sun, and Y. Zhou, "Event-triggered cooperative adaptive fuzzy control for stochastic nonlinear systems with measurement sensitivity and deception attacks," *IEEE Transactions on Fuzzy Systems*, vol. 31, no. 3, pp. 774–785, 2023.
[35] Q. Yang, J. Wang, H. Shen, and J. H. Park, "Fuzzy formation control for nonlinear multiagent systems with two time scales: A reinforcement learning scheme," *IEEE Transactions on Fuzzy Systems*, vol. 32, no. 12, pp. 7190–7195, 2024.
[36] C. Yan, J. Xia, J. H. Park, and X. Xie, "Reinforcement learning-based adaptive event-triggered fuzzy control for cyclic switched stochastic nonlinear systems with actuator faults," *IEEE Transactions on Fuzzy Systems*, vol. 32, no. 3, pp. 1131–1143, 2024.
[37] Y. Zhang, M. Chadli, and Z. Xiang, "Prescribed-time formation control for a class of multiagent systems via fuzzy reinforcement learning," *IEEE Transactions on Fuzzy Systems*, vol. 31, no. 12, pp. 4195–4204, 2023.
[38] T. Yao, Y. Xu, H. Wang, X. Qiu, K. Althoefer, and P. Qi, "Multi-agent fuzzy reinforcement learning with llm for cooperative navigation of endovascular robotics," *IEEE Transactions on Fuzzy Systems*, pp. 1–11, 2025.
[39] C. S. Xia, M. Paltenghi, J. Le Tian, M. Pradel, and L. Zhang, "Fuzz4all: Universal fuzzing with large language models," in *Proceedings of the IEEE/ACM 46th International Conference on Software Engineering*, ser. ICSE '24, New York, NY, USA, 2024.
[40] B. Lin, Y. Nie, Z. Wei, J. Chen, S. Ma, J. Han, H. Xu, X. Chang, and X. Liang, "Navcot: Boosting llm-based vision-and-language navigation via learning disentangled reasoning," *IEEE Transactions on Pattern Analysis and Machine Intelligence*, vol. 47, no. 7, pp. 5945–5957, 2025.
[41] Y. Feng, X. Wang, K. K. Wong, S. Wang, Y. Lu, M. Zhu, B. Wang, and W. Chen, "Promptmagician: Interactive prompt engineering for text-to-image creation," *IEEE Transactions on Visualization and Computer Graphics*, vol. 30, no. 1, pp. 295–305, 2024.
[42] M. Wang, M. Wang, X. Xu, L. Yang, D. Cai, and M. Yin, "Unleashing chatgpt's power: A case study on optimizing information retrieval in flipped classrooms via prompt engineering," *IEEE Transactions on Learning Technologies*, vol. 17, pp. 629–641, 2024.
[43] A.-T. Nguyen, T. Taniguchi, L. Eciolaza, V. Campos, R. Palhares, and M. Sugeno, "Fuzzy control systems: Past, present and future," *IEEE Computational Intelligence Magazine*, vol. 14, no. 1, pp. 56–68, 2019.
[44] Y. W. Hadi, L. Hof, B. Jayawardhana, and B. Haghighat, "Developing simulation models for soft robotic grippers in webots," in *2025 IEEE 8th International Conference on Soft Robotics (RoboSoft)*, 2025, pp. 1–7.
[45] X. Lin, N. Jha, M. Joshi, N. Karapetyan, Y. Aloimonos, and M. Yu, "Oystersim: Underwater simulation for enhancing oyster reef monitoring," in *OCEANS 2022, Hampton Roads*, 2022, pp. 1–6.
[46] X. Lin, N. J. Sanket, N. Karapetyan, and Y. Aloimonos, "Oysternet: Enhanced oyster detection using simulation," in *2023 IEEE International Conference on Robotics and Automation (ICRA)*, 2023, pp. 5170–5176.
[47] X. Lin, N. Karapetyan, K. Joshi, T. Liu, N. Chopra, M. Yu, P. Tokekar, and Y. Aloimonos, "Uivnav: Underwater information-driven vision-based navigation via imitation learning," in *2024 IEEE International Conference on Robotics and Automation (ICRA)*, 2024, pp. 5250–5256.
[48] H. Choset, "Coverage of known spaces: The boustrophedon cellular decomposition," *Auton. Robots*, vol. 9, pp. 247–253, 12 2000.
[49] W. C. Chow, "Brownian bridge," *WIREs Comput. Stat.*, vol. 1, no. 3, p. 325–332, Dec. 2009.
[50] A. Xu, C. Viriyasuthee, and I. Rekleitis, "Efficient complete coverage of a known arbitrary environment with applications to aerial operations," *Auton. Robots*, vol. 36, no. 4, p. 365–381, Apr. 2014.
[51] J. S. Horne, E. O. Garton, S. M. Krone, and J. S. Lewis, "Analyzing animal movements using brownian bridges," *Ecology*, vol. 88, no. 9, pp. 2354–2363, 2007.